JOURNAL OF THE PHYSICAL SOCIETY OF JAPAN, Vol. 24, No. 5, MAY, 1968

Magnetization and Magnetic Structure of Mn-Zn and Mn-Zn-Ga Alloys of CsCl-Type Structure

Tomiei HORI, Yasuaki NAKAGAWA

Department of Physics, Faculty of Science, Gakushuin University, Mejiro, Tokyo

and

Junji SAKURAI*

Chalk River Nuclear Laboratories, Atomic Energy of Canada Limited, Chalk River, Ontario, Canada

(Received November 13, 1967)

The β_1 phase of the CsCl-type structure in Mn-Zn system, which exhibits strong ferromagnetism at room temperature, was found to be stable below 175°C. Its homogeneity range extends from 50 to 56.5 at.% Mn. A canted spin structure, *i.e.* a coexistence of ferromagnetic and antiferromagnetic moments which are orthogonal to each other, was revealed to exist by the technique of neutron diffraction. Both moments decrease with increasing Mn content. An attempt to substitute a third element for Zn or Mn was unsuccessful except for Ga. The β_1 phase can contain as much as 10% Ga. The substitution of Ga for Zn gives rise to an increase in ferromagnetic moment and a decrease in antiferromagnetic moment.

§ 1. Introduction

Since the discovery of a new ferromagnetic phase in the Mn-Zn system, named the β_1 phase,[1] the present authors and their collaborators have investigated its various properties.[2-5] This phase is stable in a composition range between 50 and 56.5 at.% Mn and in a temperature range below 175°C.

The β_1 phase has an ordered bcc structure of CsCl type. An ideal CsCl-type lattice is realized at an equiatomic composition in which the Mn atoms occupy a simple cubic sublattice. In spite of such a simple arrangement of the magnetic atoms, a canted spin structure is exhibited, as shown in Fig. 1.[2,3] Each magnetic moment μ is composed of a ferromagnetic component μ_F and an antiferromagnetic component μ_{AF} which are orthogonal to each other.

When the Mn content is higher than 50 at.%, the excess Mn atoms occupying the Zn site may have a different magnetic moment from other Mn atoms occupying the Mn site and may give rise to a change in μ_F and μ_{AF} of the Mn sublattice. The change in μ_F and μ_{AF} may also occur when a third element is partly substituted for Mn or Zn, even if the substituted element is nonmagnetic. Various elements such as Ti, V, Cr, Fe, Co, Ni, Cu, Ga, Ag, and Pd were examined, but their solid solubilities in the β_1 phase were extremely small except for Ga. Thus, the detailed studies on the ternary systems were limited to Mn-Zn-Ga. The results of the magnetic measurements and the X-ray and neutron

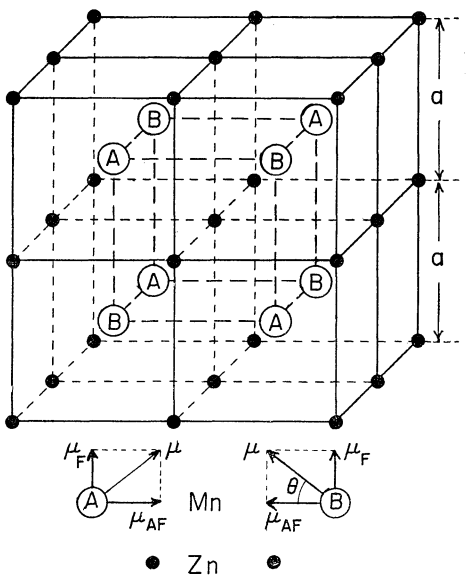

Fig. 1. Magnetic unit cell of β_1-MnZn. The magnetic moment is composed of the ferromagnetic component μ_F and the antiferromagnetic component μ_{AF}, θ being the canting angle.

* National Research Council of Canada Fellow from Research Reactor Institute, Kyoto University. Now at Hiroshima University.

diffraction experiments for Mn-Zn and Mn-Zn-Ga alloys will be reported here.

§ 2. Experimental Procedures and Results

2.1. *Preparation of specimens*

The preparation of β_1-Mn-Zn alloys is complicated because of their instability above 175°C. A high temperature phase, *i.e.* the ε phase, of the Mn-Zn system in this composition range has an hcp structure. The ε-Mn-Zn alloy can be prepared by melting Mn and Zn sealed together in an evacuated quartz tube. After being homogenized at a high temperature, the ε-phase alloy is powdered by filing and then annealed at 150°C for a few days in order to obtain the β_1-phase alloy. The internal stress imposed by filing seems to accelerate the rate of transformation from ε to β_1. This procedure has also been applied to the Mn-Zn-Ga system in which the stability of the ε phase is uncertain.

In some cases the process of homogenization of the ε-phase alloy was omitted; the molten alloy was rapidly quenched to room temperature and then annealed at 150°C. This method was also satisfactory, probably because the segregation of the quenched alloy was so fine that it could be homogenized even by the 150°C annealing.

More than 40 kinds of alloys were prepared by using 99.9% Zn, 99.999% Ga and electrolytic Mn of 99.9% purity. The mixing ratios of the specimens are illustrated in Fig. 2. The composition was determined by chemical analysis for some specimens, the results being not different from the mixing ratio by more than 0.5%, and also that there are no appreciable impurities.

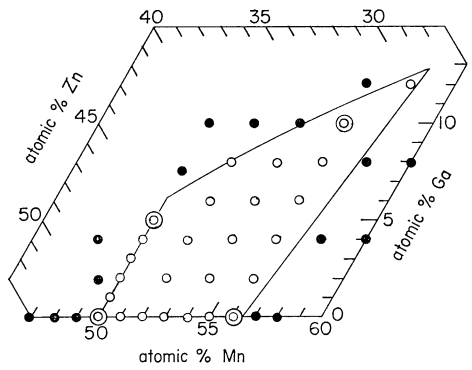

Fig. 2. Phase boundaries of β_1 phase in Mn-Zn-Ga system. Alloys examined are indicated by open and closed circles which correspond, respectively, to single β_1 phase and to mixed phases. Alloys indicated by double circles are used for neutron diffraction experiments.

The powder specimens thus obtained were used for X-ray and neutron diffraction and also for magnetization measurements. A bulk specimen of the β_1 phase can hardly be obtained because of sluggishness of the transformation. None of the usual cold-working techniques can make the internal stress large enough to accelerate the transformation rate. However, the neutron irradiation proved to be effective to produce the bulk β_1-phase specimen.*

2.2. *Phase boundaries and lattice parameters*

The homogeneity range of the β_1 phase in the ternary Mn-Zn-Ga system is shown in Fig. 2. In the binary Mn-Zn system, a Zn-rich phase is the α' phase with an ordered fcc structure of Cu_3Au type and a Mn-rich phase is the β_{Mn} phase with a complex cubic structure. The β_1 phase decomposes into $\alpha'+\beta_{Mn}$ above 175°C. Details of the present investigation of the phase diagram of the Mn-Zn system will be published elsewhere since Hansen's phase diagram[6] has to be revised in many respects.

It is to be noted here that there is another CsCl-type phase called the β phase in the Mn-Zn system, which is stable above 600°C in a concentration range near 60 at. % Mn.** This phase can be quenched to room temperature and shows similar magnetic properties to the β_1 phase.[7]

Lattice parameters at room temperature were determined using an X-ray diffractometer; NaCl powders were mixed with the specimen as a standard. The results are shown in Fig. 3. As can be seen in the figure, the phase boundaries in the binary system can be determined from the composition dependence of the lattice constant. However, this method is not applicable to the ternary system. The boundaries shown in Fig. 2 should not be regarded as very precise.

2.3. *Magnetization*

The β_1 phase exhibits a spontaneous magnetization at room temperature. The magnetization was measured using a Faraday-type magnetic balance. Its composition dependence at room temperature is shown in Fig. 4. The higher the

* The authors are indebted to Dr. N. Tamagawa of Research Laboratory of Sony Corporation for carrying out the irradiation experiments.

** As a matter of fact, the name of the β_1 phase was due to its similarity to the β phase which had been found and named several decades before.

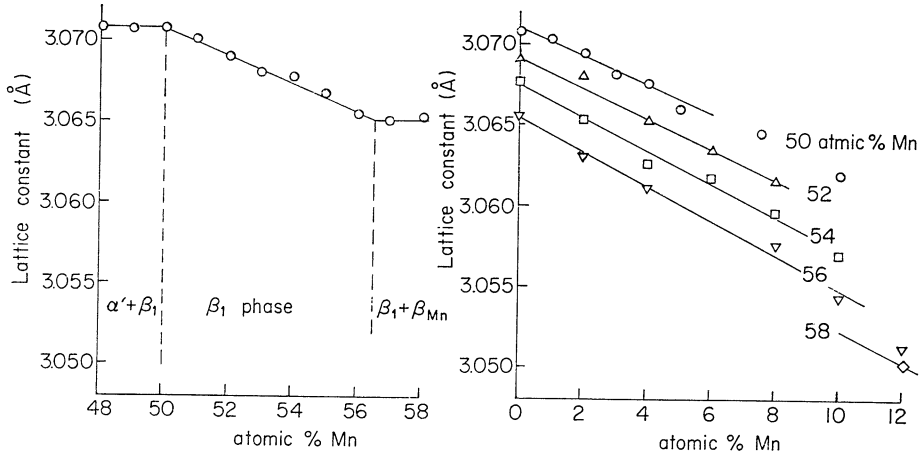

(a) Binary Mn-Zn alloys (b) Ternary Mn-Zn-Ga-alloys

Fig. 3. Lattice constants at room temperature.

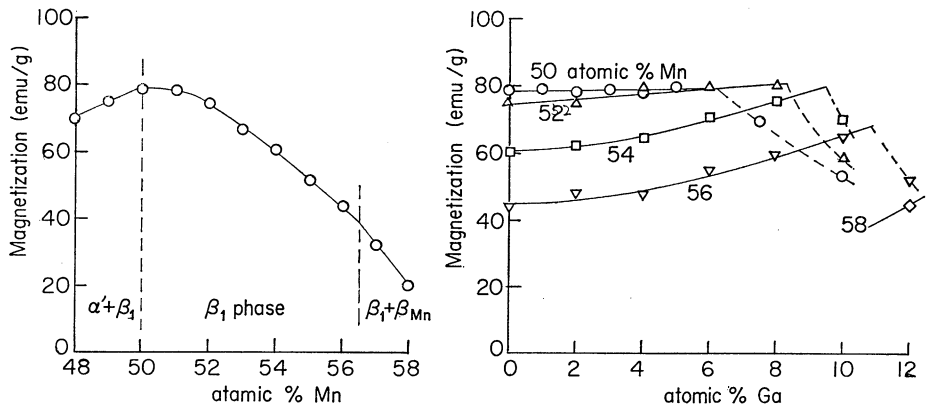

(a) Binary Mn-Zn alloys (b) Ternary Mn-Zn-Ga alloys

Fig. 4. Magnetizations in a field of 10 kOe at room temperature.

Mn content, the smaller becomes the magnetization. The substitution of Ga for Zn gives rise to an increase in magnetization.

Typical examples of the field dependence up to 14 kOe and the temperature dependence down to liquid nitrogen temperature are shown in Figs. 5a and 5b, respectively.* The Curie point is considerably higher than 450°K, at which this phase begins to decompose. For the alloys with excess Mn, the approach to saturation is more difficult and the extrapolated Curie point seems to be higher.**

* The experiments in stronger fields and at lower temperatures are now in progress and will be reported later.

** The extrapolation of the curves in Fig. 5b is very rough. However, the temperature dependence of the nuclear magnetic resonance frequency of Mn^{55} in β_1-$Mn_{50}Zn_{50}$ could be measured up to 510°K,[4] from which the Curie point is estimated as 670±50°K.

2.4. *Neutron diffraction*

Powder patterns of neutron diffraction were taken at Chalk River NRX Reactor. The specimens examined were $Mn_{50}Zn_{50}$, $Mn_{56}Zn_{44}$, $Mn_{50}Zn_{45}Ga_5$, and $Mn_{56}Zn_{34}Ga_{10}$. Experimental procedures and the results for $Mn_{50}Zn_{50}$ had already been reported in ref. 2. A vanadium cassette was used for a general survey because of smallness of its coherent scattering cross section. The (110) scattering of vanadium, however, was not completely negligible, superposing to the (110) line of the β_1 phase. Thus, an aluminum cassette was also used in order to correct the error.

The diffraction pattern obtained was similar to that shown in Fig. 6 in ref. 2. There was no remarkable difference in the pattern between room temperature and liquid nitrogen temperature. Relative intensities I_{obs} of the diffraction lines at room temperature are tabulated in

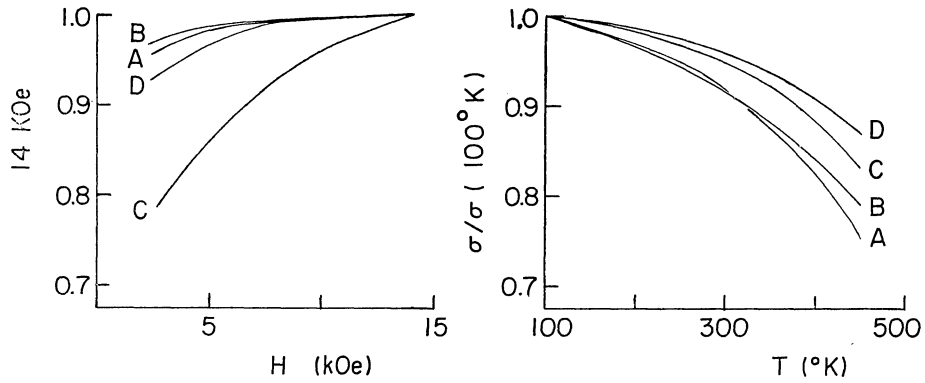

(a) Field dependence at room temperature (b) Temperature dependence in a field of 10kOe

Fig. 5. Magnetizations of β_1-phase alloys: (A) $Mn_{50}Zn_{50}$, (B) $Mn_{50}Zn_{45}Ga_5$, (C) $Mn_{56}Zn_{44}$, (D) $Mn_{56}Zn_{36}Ga_8$.

Table I. Neutron diffraction intensities and the magnetic moments (in Bohr magneton) of β_1-phase alloys.

	$Mn_{50}Zn_{50}$		$Mn_{50}Zn_{45}Ga_5$		$Mn_{56}Zn_{44}$		$Mn_{56}Zn_{34}Ga_{10}$	
(hkl)	I_{calc}	I_{obs}	I_{calc}	I_{obs}	I_{calc}	I_{obs}	I_{calc}	I_{obs}
$(\frac{1}{2}\frac{1}{2}\frac{1}{2})$ I_{AF}	54	54	48	48	37	37	34	34
(100) $\{I_N$	100	109	102	111	77	80	82	87
(100) $I_F\}$	9		9		3		5	
(110) $\{I_N$	7	12	8	12	2	5	3	6
(110) $I_F\}$	6		6		2		3	
$(\frac{3}{2}\frac{1}{2}\frac{1}{2})$ I_{AF}	18	14	16	13	12	11	11	9
(111) $\{I_N$	52	50	53	47	40	33	42	37
(111) $I_F\}$	2		2		1		1	
(200) $\{I_N$	2	2	2	2	1	0	1	0
(200) $I_F\}$	1		1		0		0	
$(\frac{3}{2}\frac{3}{2}\frac{1}{2})$ I_{AF}	7	4	6	4	5	4	4	2
(210) $\{I_N$	113	94	116	87	88	63	93	67
(210) $I_F\}$	2		2		1		1	
μ_F	1.72		1.72		1.09		1.36	
μ_{AF}	2.96		2.79		2.46		2.35	
μ	3.4		3.3		2.7		2.7	
θ	30°		32°		24°		30°	

Table I where the Miller indices are based on the chemical unit cell. The lines with half-integer indices come from magnetic moments aligned antiferromagnetically.

Effects of magnetic fields on the neutron diffraction were not examined in the present investigation. On $Mn_{50}Zn_{50}$, however, the detailed studies were made to confirm the canted spin structure.[3] When a field is applied along the scattering vector, the contribution of the ferromagnetic scattering to the diffraction lines with integer Miller indices vanishes completely whereas the intensities of the lines with half-integer Miller indices increase by 50 percent since the antiferromagnetic component is orthogonal to the ferromagnetic one.

An analysis of the diffraction intensities was made on the basis of the following assumptions. (1) Nuclear scattering length, $b_{Mn}=-0.36$,[8] $b_{Zn}=0.61$,[9] and $b_{Ga}=0.72$[9] in 10^{-12} cm. (The value for Zn is somewhat different from that used previously.[2,8]) (2) One sublattice of the CsCl-type lattice is occupied exclusively by Mn, and the other by Zn, Ga, and excess Mn (if they exist). There is no higher-order superlattice. (3) The magnetic structure of the Mn-sublattice is the same as that shown in Fig. 1. (4) The Zn-sublattice has no magnetic moment even if

there are excess Mn atoms. (5) The magnetic form factors are the same as those for MnSb.[10]

Calculated intensities I_{calc} are also tabulated in Table I, which are normalized to the nuclear part I_N of the (100) line of $Mn_{50}Zn_{50}$. Ferromagnetic contributions I_F are calculated from the ferromagnetic moment μ_F determined from the magnetization. Observed intensities I_{ob} for each alloy are normalized so that the total intensity of the (100) line agrees with the calculated one. Then the antiferromagnetic moment μ_{AF} is determined so that the calculated intensity I_{AF} of the $(\frac{1}{2}\frac{1}{2}\frac{1}{2})$ line agrees with the observed one. Total magnetic moment μ and the canting angle θ (see Fig. 1) are calculated from μ_F and μ_{AF}, and also listed in Table I.

In general, I_{obs} is less than I_{calc} for the lines with higher Miller indices since the Debye temperature factor was ignored in the present calculation. The assumption (2) aforementioned is justified because I_{calc} is in good agreement with I_{obs} for the (110) line which is very sensitive to the atomic ordering.

The assumption (4) may require some explanations. The excess Mn atoms may possibly have a magnetic moment aligned antiparallel to the ferromagnetic component of the Mn-sublattice because the magnetization is decreased with an increase of Mn content. This magnetic moment, if it exists, contributes to the lines with integer Miller indices; the intensities of (100) and (111) are proportional to $(\mu_F+c\mu')^2$ while those of (110) and (200) to $(\mu_F-c\mu')^2$, where μ' and c denote, respectively, the magnetic moment and the concentration of excess Mn in the Zn-sublattice. Since the magnetization is also proportional to $(\mu_F-c\mu')$, the calculated values of I_F of (110) and (200) remain unaltered. The values of I_F of (100) and (111) increase appreciably, but this is unimportant because I_N is much larger than I_F for these lines. Thus, the neglect of $c\mu'$ gives no serious errors in determining the value of μ_{AF} although the values of μ_F, μ and θ are dependent on $c\mu'$.

§ 3. Discussion and Conclusions

Lattice constants and magnetizations of the β_1-phase alloys are summarized in Fig. 6, where contours of these quantities are drawn. The lattice constants are almost uniquely determined by the Zn content, whereas the magnetizations are mainly dependent on the Mn content. The gradient of magnetization almost vanishes when the Mn content approaches 50 at.%. The antiferromagnetic moment shown in Table I also decreases with increasing Mn content. An addition of Ga to the Mn-rich alloy causes an increase in magnetization and a decrease in antiferromagnetic moment.

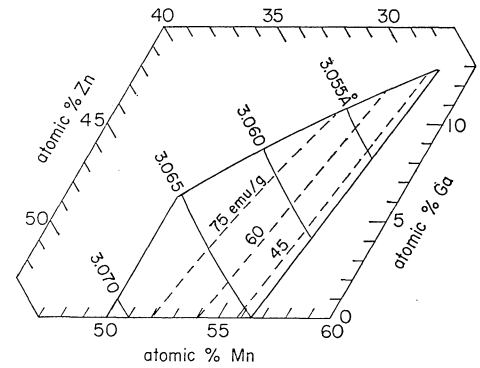

Fig. 6. Contours of lattice constants (solid lines) and magnetizations (broken lines) of β_1-phase Mn-Zn-Ga alloys.

Before interpreting these results, the origin of the spin canting in the Mn-sublattice must be discussed. Neither a conical screw structure due to a strong anisotropy and long-range exchange interactions[11] nor a canted spin structure due to an antisymmetrical spin coupling[12] can be exhibited in such a simple lattice with high symmetry. An existing theory which accounts for the spin canting in the β_1 phase may be de Gennes' theory based on the double exchange interaction.[13] The interaction energy between the two spins is expressed as

$$E=-a\cos\varphi-b\cos\frac{\varphi}{2}, \qquad (1)$$

where a and b are coefficients of the usual exchange and the double exchange, respectively, and φ is an angle between the two spins. If a is negative (antiferromagnetic) and b is positive, E becomes minimum at $\varphi=2\cos^{-1}|b/4a|$. The canting angle θ is a half of φ, and so

$$\left.\begin{array}{ll}\theta=\cos^{-1}|b/4a| & \text{if } b<4|a|,\\ \theta=0 & \text{if } b>4|a|.\end{array}\right\} \qquad (2)$$

However, no sufficient justification has yet been found for this model.

Excess Mn atoms in the Zn-sublattice may have magnetic moments which are aligned antiparallel to μ_F and reduce the magnetization. It is more likely, however, that the excess Mn atoms strongly interact on the nearest neighbour Mn atoms in the Mn-sublattice so that they lose

their magnetic moments as in the case of covalent bonding. This consideration, based on the fact that most of Mn-rich alloys show Pauli paramagnetism or antiferromagnetism with small magnetic moments, may give an acceptable explanation of the assumption (4) in §2.4, and may also account for the decrease of μ in the Mn-rich alloys shown in Table I.

An addition of Ga in β_1-Mn-Zn gives no appreciable effect on μ but reduces the canting angle θ. This may be related to the fact that the substitution of trivalent Ga for divalent Zn results in an increase in conduction electron density. The canting angle θ is determined by various magnetic interactions which may more or less depend on the conduction electrons. The dependence of θ on the concentration of excess Mn is opposite to that of Ga. This can be understood if the valency of the Mn ions is assumed to be less than two.

Acknowledgements

The authors would like to thank Dr. A.D.B. Woods and Dr. G. Dolling of AECL for their advice in the neutron diffraction experiments. This work has been supported by the Grant-in-Aid from the Ministry of Education and also by the RCA Research Grant in Japan.

References

1) T. Hori and Y. Nakagawa: J. Phys. Soc. Japan **19** (1964) 1255.
2) Y. Nakagawa and T. Hori: J. Phys. Soc. Japan **19** (1964) 2082.
3) T. Hori, Y.Nakagawa and Y. Ishikawa: J. Phys. Soc. Japan **21** (1966) 2080.
4) T. Hihara, E. Hirahara and Y. Nakagawa: J. Phys. Soc. Japan **20** (1965) 1742.
5) S. Matsuyama, Y. Nakagawa and H. Nosé: J. Phys. Soc. Japan **24** (1968) 207.
6) M. Hansen: *Constitution of Binary Alloys* (Mc Graw-Hill, 1958) 962.
7) Y. Nakagawa, S. Sakai and T. Hori: J. Phys. Soc. Japan **17** (1962) Suppl. B-I 168.
8) G. E. Bacon: *Neutron Diffraction* (Clarendon Press, 1962) 31.
9) J. W. Cable, W. C. Koehler and E. O. Wollan: Phys. Rev. **136** (1964) A240.
10) W. J. Takei, D. E. Cox and G. Shirane: Phys. Rev. **129** (1963) 2008.
11) T. Nagamiya: J. appl. Phys. **33** (1962) 1029.
12) T. Moriya: Phys. Rev. **120** (1961) 91.
13) P.-G. de Gennes: Phys. Rev. **118** (1960) 141.